Preparation and Characterization of Cellulose/Silk Fibroin Composites Microparticles for Drug Controlled-Release Applications

Suchai Tanisood , Yodthong Baimark , Prasong Srihanam *

Posted Date: 19 September 2024

doi: 10.20944/preprints202409.1442.v1

Keywords: blue dextran; cattail; cellulose; microparticle; silk fibroin; water-in-oil emulsification-diffusion

Article

Preparation and Characterization of Cellulose/Silk Fibroin Composites Microparticles for Drug Controlled-Release Applications

Suchai Tanisood, Yodthong Baimark and Prasong Srihanam *

Biodegradable Polymers Research Unit, Department of Chemistry and Centre of Excellence for Innovation in Chemistry, Faculty of Science, Mahasarakham University, Mahasarakham 44150, Thailand

* Correspondence: prasong.s@msu.ac.th; Tel.: +66-845119244

Abstract: Microparticles derived from biomaterials are becoming increasingly popular for various applications, particularly in drug delivery systems. In this study, the water-in-oil (W/O) emulsification-diffusion method was used to create cellulose (C), silk fibroin (SF), and C/SF composite microparticles. We then observed the morphology of all obtained microparticles using scanning electron microscopy (SEM), evaluated their functional groups using attenuated total reflection Fourier transform infrared spectroscopy (ATR-FTIR), and conducted thermogravimetric analysis using a thermogravimetric analyzer (TGA). SEM micrographs indicated that the native SF microparticles have the highest spherical shape with smooth surfaces. With blue dextran, the C microparticle was smaller compared to the native microparticle, while the drug-loaded SF microparticles were bigger than the native microparticle. The morphological surfaces of the C/SF composite microparticles were varied in shape and surface depending on the C/SF ratio used. The spherical shape of the C/SF composite microparticle was increased as SF content increased. Furthermore, the size of drug-loaded C/SF composite microparticles was gradually increased by the SF content. The significant functional groups in the C and SF structures were identified based on the ATR-FTIR data, and a suggestion was made regarding the interaction between the functional groups of each polymer. When compared to both native polymers, the C/SF composite microparticles exhibit improved thermal stability. The C/SF composite microparticle at a 1:3 ratio had the lowest drug release content, whereas the hydrophilicity of the C microparticle affected the highest drug release content. As a result, one crucial factor affecting the medication released from the microparticle is its thermal stability. According to the obtained results, C, SF, and C/SF composite microparticles show promise as delivery systems for drugs with controlled release.

Keywords: blue dextran; cattail; cellulose; microparticle; silk fibroin; water-in-oil emulsification-diffusion

1. Introduction

Recently, the Sustainable Development Goals (SDGs) policy has an attractive strategy to decrease the consumption of petrolium-based synthetic materials, as it is the main cause of environmental crises [1,2]. Utilizing biodegradable materials is one of the interesting ways to replace those synthetic materials according to their eco-friendly, renewable nature, low cost, and wide availability [3,4]. The development of biodegradable materials has been performed for many applications, including food packaging [5–7], delivery systems [8], and biomedical products [9]. Cellulose and silk fibroin are two of the most interesting biopolymers among biodegradable materials that are regularly explored. Their sustainable sources and characteristics provide the most compelling argument.

The most prevalent biopolymer is cellulose, a fiber of glucose units connected by β -1,4-glycosidic linkages throughout its molecular structure. When it comes to biomaterials, cellulose is superior to others in a number of ways, including its capacity to adapt mechanical properties, its biodegradability, and its thermal stability [10–12]. Furthermore, cellulose can be discovered in a wide range of organisms, such as marine life, plants, algae, and bacteria [13,14]. As a result, it may be

 doi:10.20944/preprints202409.1442.v

referred to as a sustainable raw resource [15], which is also produced at a low cost. According to earlier sources, the cellulose According to earlier studies, cellulose has been created in a wide variety of forms based on its intended use [16–18]. These applications include food packaging [19,20], wastewater treatment [21], surface coating materials [22], and biomedicine [23].

The natural protein-based polymer identified as silk is spun into fibers by silkworms to generate silk cocoons. The two major components of silk fibers are fibrous silk fibroin and globular silk sericin. The glue-like protein sericin covers the main fiber called "silk fibroin (SF)" [24,25]. The silk sericin was typically thrown away as waste during the degumming procedure at the end of the silk yarn production process. Because of its biodegradable and biocompatible characteristics, the SF is taken into consideration for potential construction in the biomaterial category [26]. SF-based devices have drawn a lot of interest for a variety of applications [27,28]. Additionally, the SF was processed to create a number of bioactive scaffolds [29].

In previous works, the microparticle derived from biopolymers has been attractively interested, according to which they were suggested as potential devices for various fields [30]. Because of their clearly established model for degradation and release profile, biodegradable microparticles are frequently targeted for use as controlled-release vehicle [31–33]. There have been several reported methods for producing microparticles [34]. Each method has its own distinct advantages. We have developed the microparticles from various bio-polymers at our research unit adopting the water-in-oil (W/O) emulsification-diffusion technique. We also been reported about optimal conditions and properties of the SF microparticles, either with and without additional biopolymers [32,33,35]. Furthermore, our earlier work also produced cellulose microparticles [36]. Nevertheless, there are other aspects that need to be improved, and the cellulose microparticles that were produced weren't up to the requirements of the perfect protocol. In addition, SF mixed cellulose microparticles never been developed by previous information. With that in consideration, the purpose of this study is to prepare the cellulose (C), SF, and C/SF/ composite microparticles employing the water-in-oil (W/O) emulsification-diffusion method. Stirring rate, volume of SF, C, and SF/C, and W/O volume ratios were studied for gathering data. The SF solution in this work was made by dissolving *Bombyx mori* silk cocoons in a tertiary mixture solution of $CaCl_2$:Ethanol:H_2O (1:2:8 by mol). Cattail raw materials were chemically treated to provide cellulose. It was established how different parameters affected the microparticles' size, shape, and conformational change. Additionally, the solubility of the microparticles was examined and discussed.

2. Materials and Methods

2.1. Materials

The cocoons of *B. mori* silk were provided by the Silk Innovation Center at Mahasarakham University, located in the Khamriang sub-district of Kantharawichai, Maha Sarakham, Thailand, and the cattail (*Typha angustifolia* L.) trees were gathered from a pool. The cattail tree was chopped off 10 cm from the rhizome and 15 cm from the tip. Tap water was then used to remove some dirt, and the tree was left to dry at room temperature. The samples were crushed and stored in plastic bags once they had dried. We purchased chemicals from Merck Life Science Private Ltd. (Maharashtra, India), LOBA CHEMIE PVT. Ltd. (Maharashtra, India), and Kemaus (New South Wales, Australia) in that order: sulfuric acid (H_2SO_4), sodium hypochlorite (NaClO), and sodium hydroxide (NaOH). We obtained ethanol (C_2H_5OH), sodium carbonate (Na_2CO_3), and sodium chloride (NaCl) from Merck KGaA company (Darmstadt, Germany) and Ajax Finechem Pty Ltd. (Auckland, New Zealand). Before use, none of the reagent-grade chemicals used in this study required additional purification.

2.2. Extraction of Cellulose

The gathered cattail samples were sequencely cleaned twice with deionized water after an hour-long immersion in ethanol, before drying at 80 °C for two hours. They were then weighed to determine its exact weight. The step of cellulose extraction was followed with the previous report [36]. Briefly, the 10g samples were boiled in 100 mL of 4% NaOH for four hours. After that, the

 doi:10.20944/preprints202409.1442.v

reaction was stopped by filtration. After that, the solid samples were washed with distilled water to reach a neutral pH. In order to bleach the neutral samples, 2% (v/v) sodium hypochlorite (NaClO) was added and heated to 80 °C for two hours. After that, the reaction mixture was centrifuged to exclude residue. Subsequently, the reaction mixture was hydrolyzed with 5% H_2SO_4 at 50 °C for three hours. The resulted mixture was then filtered, washing with distilled water to neutral pH. Finally, cellulose was obtained and stored it in a refigurator until further processing.

2.3. Preparation of Silk Fibroin Solution

The silk fibroin (SF) was derived from Thai silk *B. mori* cocoons (Nang Lai variety). After being gathered, the cocoons were cleaned and then chopped into small segments. In order to eliminate silk sericin, they were then boiled twice in a 0.5% (w/v) Na_2CO_3 solution for 30 minutes each time at 100 °C. The degummed silk samples were then rinsed with distilled water until the pH level was neutral in order to obtain SF. After that, the SF was dissolved for 60 minutes at 75 °C with continuous stirring using a tertiary solvent system that consists of $CaCl_2$:Ethanol:H_2O (1:2:8 by mol). Using a dialysis membrane (MW cut off 10 kDa, Thermo Scientific, Massachusetts, USA), the hydrolysate SF was dialyzed against distilled water for three days to exclude any salt. The concentration of the SF solution was then calculated, and distilled water was added to get it down to 2% (w/v).

2.4. Preparation of C, SF and C/SF Blend Microparticles

In this work, All of the microparticles were produced using the water-in-oil (w/o) emulsification diffusion method [30]. The C and SF solutions were used as the water phase, and ethyl acetate was depicted as the oil phase. The form, size, and characteristics were influenced by many parameters, including as the volume, concentration, and rate of stirring of polymers, as well as W:O ratios that were examined. The stirring rate was set up in the range of 600-800 rpm, and concentrations of the polymers were tried out at 0.5-1.5% (w/v). In the preparation step, the oil phase, ethyl acetate, contained in a container, was stirred on the magnetic stirrer apparatus. After that, a suitable volume of each polymer solution was gradually added to the solvent dropwise while stirring was maintained for 30 minutes. Moreover, the C/SF blend microparticles were also constructed by the same method firstly described. Using constant conditions, a desirable SF solution volume and concentration have been identified for blending with C solution. The different C/SF mixed ratios of 3/1, 1/1, and 1/3 (v/v) were prepared before use and stirred for 30 minutes to achieve homogenous solutions. In order to prevent the solvent from evaporating throughout the emulsification and diffusion processes, aluminum foil was placed over the beaker. Afterwards the particles were gathered by centrifugation, the solvent was completely evaporated and they were dried at room temperature in a vacuum oven.

2.5. Preparation of Drug-Loaded Microparticles

In order to observe the drug release profile, the microparticles loaded with blue dextran were also created. In summary, prior to construction, each polymer solution (0.0025 g/1 mL) contained the water-soluble drug blue dextran. Next, for 30 minutes, the combined solution was slowly dropped into 100 mL of ethyl acetate while being stirred at 700 rpm. After being separated by centrifugation, the drug-loaded microparticles were allowed to dry at room temperature in a vacuum oven.

2.6. An Analysis of the Microparticles' Characters

2.6.1. Morphology Observation

A scanning electron microscope (SEM) was used to investigate the morphology of each created microparticle. An aluminum stub was used for each type of microparticle. All examined microparticle surfaces were subjected to an electron-exciting Au sputter coating before being examined under a 15 kV.

 doi:10.20944/preprints202409.1442.v

2.6.2. Analysis of Functional Group

The functional groups of the produced microparticles were examined using an attenuated total reflectance (ATR) accessory on a Fourier transform infrared (FTIR) spectrometer (Perkin Elmer-Spectrum Gx, USA). The results of the ATR-FTIR spectrum were obtained by using 32 scans and a range between 4000-400 cm1 of wavenumber at a spectral resolution of 4 cm1. This process was managed by using air as the reference.

2.6.3. Thermal Stability

The thermal stability of the constructed microparticles was investigated using a thermogravimetric analyzer (TGA) (SDTQ600, TA-Instrument Co. Ltd., New Castle, DE, USA). The microparticles were put inside an aluminum pan and heated at a fixed rate of 20 °C per minute between 50 and 800 °C. The procedure was carried out in a nitrogen-filled atmosphere. There were numerous weight losses documented over time.

2.6.4. Drug Release Analysis

At room temperature, the mixed microparticles of cellulose and blue dextran were submerged in distilled water while being shaken. 2.5 mL of water was collected after the intervals of 1, 2, 3, 4, 8, 16, 24, and 48 hours. The absorbance at 640 nm was then measured after the collected volume was replaced with the same fresh volume of water. By comparing the concentration of blue dextran released from the mix microparticles to a standard curve, the concentration was estimated.

3. Results and Discussion

3.1. Morphological Observation

3.1.1. Cellulose Microparticles

The cellulose content extracted from cattail trees was 17.88 ± 0.61%. This amount was in the range content with previous reports [17,37]. The method for producing biopolymer microparticles using water-in-oil emulsion diffusion has been published previously by our research group. A number of variables, including the volume of each polymer, the speed of stirring, the ratio of the water (W) phase to the oil (O), and surfactants and crosslinking agents, all had an influence on the success of the microparticle production process [27,31,34]. The spherical shape of the microparticles is appropriate for application as a drug delivery device since it allows them to be easily and promptly transported throughout the bodily fluid. Additionally, the spherical form has direction balance and might hold components that being released in any direction [32,35]. Figure 1a illustrates the morphology of the 2.5% cellulose microparticles that were created. The prepared microparticles have a size in the range of 60-700 µm, with the largest distribution being 60-100 µm, followed by 200-500 µm. The results clearly illustrate that the manufactured microparticles have a somewhat complete appearance. It is possible to create completely spherical microparticles under these conditions. The C microparticles have a smooth surface and are packed closely together by chemical bond formation [38]. However, it was found that the particles' surface significantly wrinkle. Water evaporation while drying was thought to be the cause of this [39]. At low magnification, it was found that the particles were not dispersed equally.

A hydrophilic substance called blue dextran was selected in order to investigate the effects of C microparticles on drug encapsulation. Figure 1b shows the morphological outcomes of the blue dextran-containing cellulose microparticles. The findings showed that although the microparticles were fully formed, they were not spherical as desired. The microparticles have an angular form in general. In comparison to the native C microparticles, blue dextran-loaded C microparticles have smaller sizes, with the largest distribution in the range of 45-80 µm and 200-400 µm. Since blue dextran is water-soluble, adding it might increase the polarity of the solution, which will interrupt the spherical form. Therefore, the spinning rate used for the microparticle construction was decreased from 700 to 600 rpm.

 doi:10.20944/preprints202409.1442.v

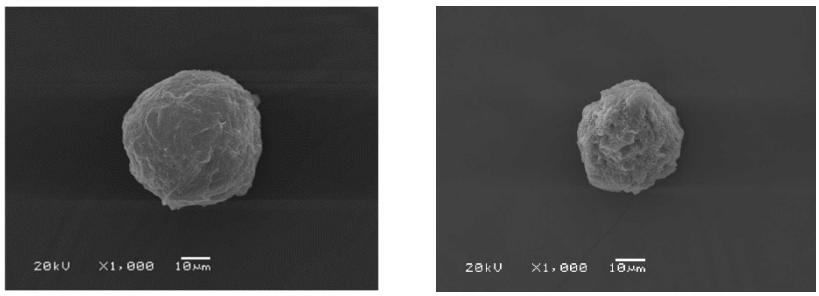

(**a**) (**b**)

Figure 1. SEM micrographs of C microparticles (a) prepared by the condition of 1 mL of 2.5% (w/v) cellulose solution, 100 mL ethyl acetate by stirring rate of 700 rpm, and blue dextran-loaded C microparticle (b) by stirring rate of 600 rpm.

3.1.2. Silk Fibroin Microparticles

Figure 2a shows an SEM micrograph of the SF microparticles. The microparticles have a spherical shape. The surface of the SF microparticle is smooth with a solid texture. At low magnification, the prepared SF microparticles had different sizes; some particles have incomplete formation and are hollow. It also has a flat, elongated shape resembling an oval. When compared with C microparticles, SF microparticles are approximately 2-2.5 times smaller. Furthermore, the size of SF microparticles, which range from 25 to 45 μm, is comparable. Figure 2b displays SF microparticles loaded with blue blue dextran. The outcome showed that the SF loaded with drug could be formed into precisely formed, spherical microparticles. Moreover, the drug-loaded SF microparticles had increased sizes into about 2 folds (45-80 μm) of the native SF. When considered in detail, it was found that the microparticles had a rough surface with irregular form. This is because the polar components of blue dextran may rapidly evaporate from the matrix. The less polar SF, on the other hand, attaches itself to the non-polar portion of blue dextran and does not evaporate. The microparticles' spherical form is mostly due to the binding of SF. The polarity of a molecule, whether high or low, plays a significant role in the shape of the particles that are obtained. Furthermore, it has been observed that stirring speed affects particle shape and size [34,35].

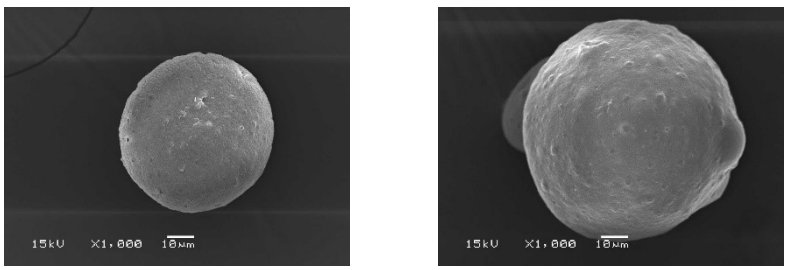

(a) (b)

Figure 2. SEM micrographs of SF microparticle (a) prepared by the condition of 1 mL of 2.0% (w/v) SF solution, 100 mL ethyl acetate by stirring rate of 700 rpm, and blue dextran-loaded SF microparticle (b) by stirring rate of 600 rpm.

3.1.3. C/SF Composite Microparticles

The C/SF composite microparticles were prepared using 2.5% C and 2% SF with different volume ratios of 3:1, 1:1, and 1:3, respectively. As seen in Figure 5, the results showed that the ratio that prepared the composite microparticles the best was 1:3. In contrast to the SF microparticles, the obtained microparticles were discovered to not be spherical. Additionally, there were some indentations on the surface that went inside, and there were a few tiny holes. It is believed that the polar components of the microparticle evaporated during drying, resulting in these holes [19,40]. The two polymers, which are not homogenous mixes, are assumed to have separated, leading to the

 doi:10.20944/preprints202409.1442.v

indentation into the microparticle. The evaporation of polar solutions and the generation of spherical particles do not occur by the same forces and times between molecules.

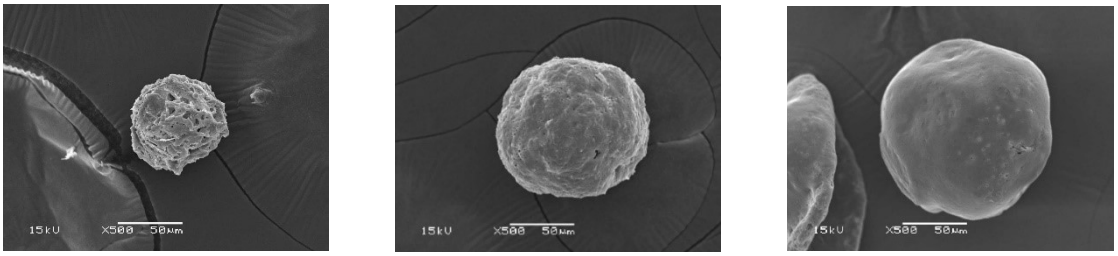

(**a**) (**b**) (**c**)

Figure 3. SEM micrographs of C/SF composite microparticles prepared by the condition of 1 mL of 2.5% C/2 % SF at 3:1 (a), 1:1 (b), 1:3 (c) solution, 100 mL ethyl acetate by stirring rate of 700 rpm.

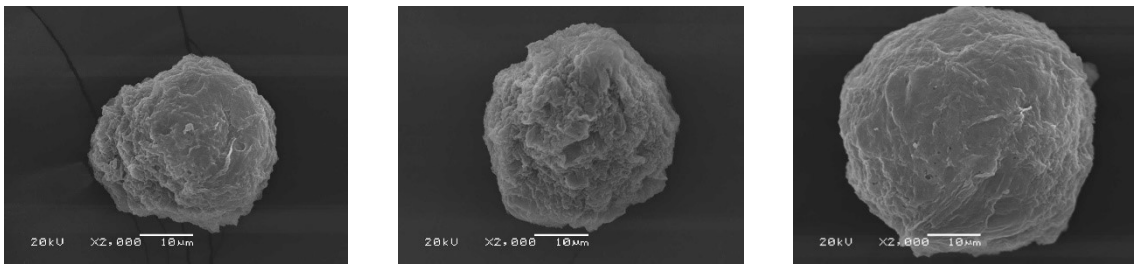

(**a**) (**b**) (**c**)

Figure 4. SEM micrographs of C/SF composite microparticles prepared by the condition of 1 mL of 2.5% C/2 % SF at 3:1 (a), 1:1 (b), 1:3 (c) solution, 0.0025g blue dextran, 100 mL ethyl acetate by stirring rate of 700 rpm at different magnifications.

3.2. FTIR Spectra of Microparticles

ATR-FTIR spectroscopy was used to investigate the functional groups of the generated microparticles, as illustrated in Figure 7. Significant functional groups of the C microparticle (Figure 7a) are considered seriously at the hydroxyl group's absorption location, which is between 3352 cm^{-1} (-OH stretching). The carbonyl ester group (C=O stretching) of hemicellulose is represented by the absorption peak in 1635 cm^{-1}, while the methyl group (-CH_2 stretching) is positioned at approximately 2850-2950 cm^{-1}. The wavelength of lignin can be found at 1300 cm1 and 1014 cm^{-1}, which correspond to the asymmetric location of glucose units and C-O-C groups joined by β-1,4 glycosidic linkages at 900 cm^{-1} [17,41,42].

The functional groups' absorption peaks in the protein structure are displayed in Figure 7e. The peptide bond, or R-COONH-R, is where amino acids are bonded to one another. The locations of the three different amide types, including amide I, are found in the range of 1700-1600 cm^{-1} in the light absorption region. The carbonyl group (-CO-) is associated with this peak; amide II can be seen in the absorption region between 1600-1500 cm^{-1}. This absorption range is associated with the amide III, methyl group (-CH), and amine group (-NH). An absorption region appears approximately 1300-1150 cm^{-1}. Absorption in this range involves groups such as -NH in the plane, -C-C-, and -CO- in the straight line, and the absorption position is approximately 1042 cm^{-1} [43,44].

Table 1 shows the FTIR spectra of the SF/C composite microparticles mixed at various ratios. The SF microparticles have a β-pleated sheet structure at both the amide I and II positions. This structure makes the particles hard, brittle, and easy to break. Cellulose exhibits strong absorption at the hydroxy group (-OH) position. This group has a strong polarity, resulting in a soft and flexible structure. Considering the composite microparticles, the light absorption value shifted and changed in a way that improved the structure's flexibility while maintaining its strength. Because of the higher concentration of silk fibroin, the microparticles remain a beta-sheet structure at the amide I and II positions [45]. This finding demonstrates the compatibility of cellulose and silk fiber and the

 doi:10.20944/preprints202409.1442.v

formation of interactions through the functional groups present in the structures of each polymer, including hydrophobic interactions, van der Waals forces van der Waals forces, and hydrogen bonds [46].

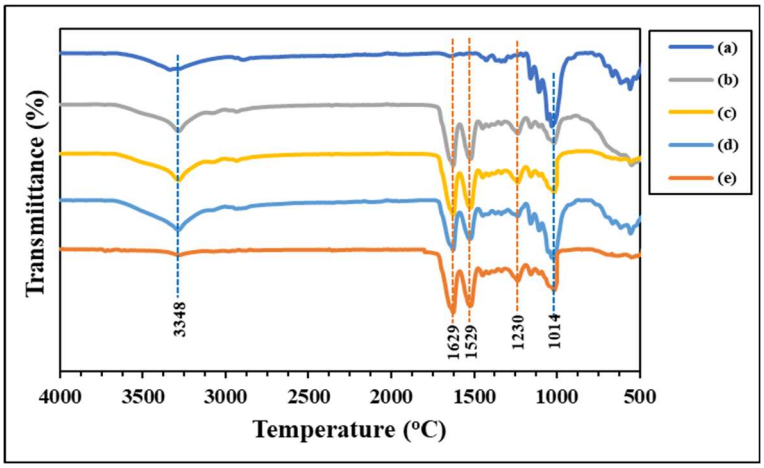

Figure 7. ATR-FTIR spectra of microparticles; native cellulose (a), C/SF composites at 3:1 (b), 1:1 (c), and 1:3 (v/v) (d) ratios, and native SF (e).

Table 1. The light absorption peaks for main function groups of different microparticles.

Types	Absorption (cm^{-1})				
	O-H Str.	C-H Str.	C=O Str.	N-H Str.	C-O Blend
Native C	3350	2899	1632	-	1018
C/SF (3:1)	3348	2928	1629	1529	1014
C/SF (1:1)	3348	2956	1629	1529	1014
C/SF (1:3)	3348	2956	1629	1529	1014
Native SF	3325	2956	1629	1529	998

3.3. Thermogravimetry Analysis

A weight loss and the maximum decomposition temperature ($T_{d,\ max}$) of the prepared microparticles across 0-800 °C were investigated using a thermogravimetric analyzer (TGA). According to the TG thermograms in Figure 8, the decomposition of the microparticles occurred in at least three stages. These stages are clarified by the DTG curves, which exhibited in Figure 9. Small peaks indicate that water evaporation [34] from the microparticles occurred at low temperatures (60-80 °C), which was the cause of the initial decomposition. This suggested that the moisture remained in low content in the microparticles. The second stages of decomposition were observed at 260-300 °C, which dominant revealed in the SF/C composite microparticles. This region is the decomposition temperature of protein [27,32,34]. The result showed that SF and C composite is not homogeneous texture comparison to the native SF. The third stage (between 300 and 400 °C) dealt with the breakdown of silk fibroin [27,32] and cellulose [47]. Compared to native polymers, the charred residue of the composite microparticles is slightly higher at the end temperature test. Apart from the composite microparticles, the C/SF ratio with a 1:3 ratio has the highest value, approximately 35%. The ratios of 1:1 and 3:1 had burned residues of 30% and 28%, respectively, after that. These charred residues did not longer degrade in the range of tested temperature. Moreover, the native C microparticle had an greater degradation at the begin of heating temperature. This due to the hydrophilic functional group in the C structure were broken and evapated in high content. Table 2 provides an overview of each microparticle's thermal behavior. Because of the establishment of robust intermolecular interactions between C and SF, the decomposition temperature of the C/SF composite microparticles increased, which gradually increased follwing by increasing of SF content. Therefore this result evidenced that C and SF are joined together via the mentioned interaction, and improving their thermal stability [48,49].

 doi:10.20944/preprints202409.1442.v

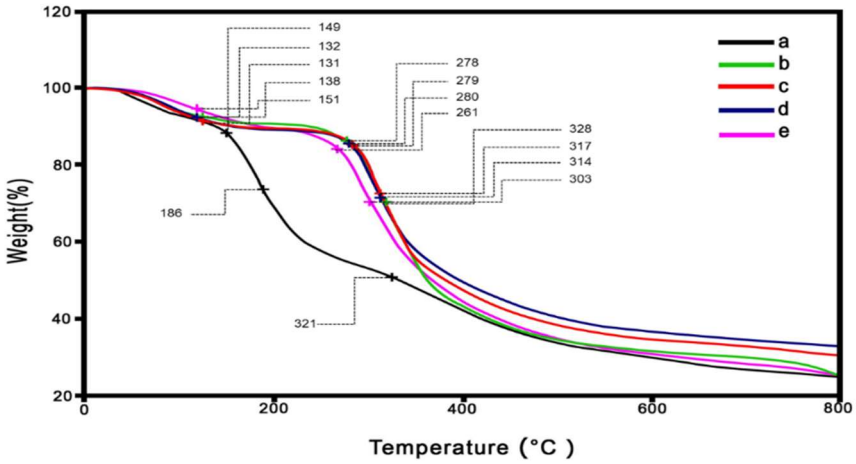

Figure 8. TG thermograms of microparticles; native cellulose (a), C/SF composites at 3:1 (b), 1:1 (c), and 1:3 (v/v) (d) ratios, and native SF (e).

Table 2. The maximum decomposition temperature of the prepared microparticles.

Types	$T_{d,\,max}$ (°C)	Charred Residue Weight at 800 °C (%)
Native C	150, 310	25
C/SF (3:1)	131, 280, 314	28
C/SF (1:1)	132, 280, 317	30
C/SF (1:3)	138, 280, 328	35
Native SF	260, 303	27

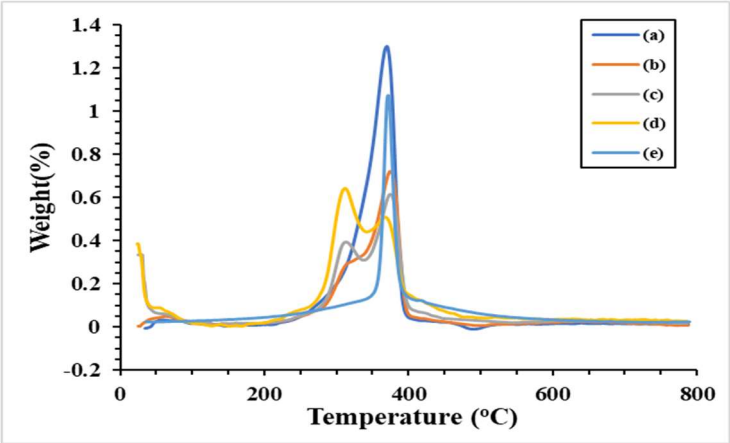

Figure 9. DTG curves of microparticles; native cellulose (a), C/SF composites at 1:3 (b), 1:1 (c), and 3:1 (v/v) (d) ratios, and native SF (e).

3.4. Releasing of Blue Dextran from Microparticles

Figure 10 shows releasing profiles of blue dextran from the prepared microparticles. The results shown that the releasing of blue dextran had dramatically released at the initial time (1 to 12 h) of experimental and then gradually increased until 24 h after testing. Considering the detail of the drug-releasing profile, the C/SF composite with a 1:3 ratio displayed the least amount of drug released, whereas the C microparticles had the most drug released. The drug release content from C/SF composite microparticles followed by the mixing ratio of 1:1, and then 3:1, respectively. The native SF microparticle released blue dextran in the second runner up from the native C microparticle. A water reaction causes the microparticles' surface texture to burst, releasing the drug-loaded microparticle. In its structure, SF contains high crystalline regions. These areas affected the microparticle's solid texture, which optimized the drug release and the microparticle's resistance to

 doi:10.20944/preprints202409.1442.v

water. Furthermore, the interaction between C and SF via different interactions improving the stability of composite microparticles as indicated from thermal stability results. Therefore, the C/SF composite microparticles can be protected the release of blue dextran in higher than both native polymers.

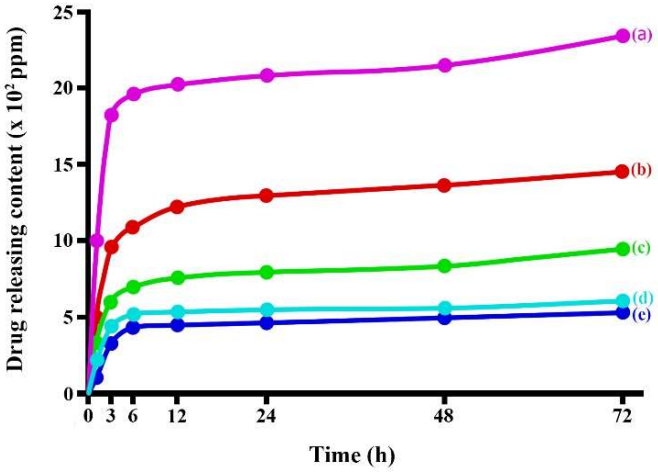

Figure 10. Releasing patterns of blue-dextran from the microparticles; native C (a), native SF (b), C/SF composites at 3:1 (c), 1:1 (d), and 1:3 (v/v) (e) ratios.

4. Conclusions

The cattail's cellulose fibers were extracted using a conventional chemical treatment method. The obtained cellulose and silk fibroin were used as raw materials for the construction of microparticles. The SF microparticles were prepared in spherical shape in easier than the C microparticles. We suggested that the morphological surfaces and shape of microparticles concerned in different parameters. SEM images revealed that the C/SF composite microparticles could also be constructed, even the mixing ratios are the main factor to give the suitable target. The C/SF composite with 1:3 mass ratio is the favor composite to receive the satisfy microparticle. ATR-FTIR spectra exhibited the main functional groups in each polymer structure. However, some light absorption peaks were shifted and appeared in the C/SF composite microparticles. This indicated that the interactions between the functional groups among C and SF were formed. These resulted to enhance the thermal stability and charred residue of the microparticles. All prepared microparticles were loaded blue dextran to study its release profile over 72 h. The obtained results showed that the release of drug content was varied by types of the prepared microparticles. The highest drug content was released from the C microparticle, while the C/SF composite microparticle at 1:3 ratio has the lowest. This suggest that the release profile depending on raw materials used for construction the microparticle, which could be adjusted the mixing ratios before microparticle preparation. In conclusion, both cellulose and silk fibroin would be promising for hydrophilic molecules loading for drug controlled-release applications.

Author Contributions: Conceptualization, P.S.; methodology, S.T. and P.S.; investigation, S.T. and P.S.; resources, Y.B.; visualization, Y.B. and P.S.; writing-original draft, S.T., and P.S.; writing, reviewing, and editing, Y.B., and P.S. After reading the published version of the manuscript, all writers have given their approval.

Funding: This research project was financially supported by Thailand Science Research and Innovation (TSRI). The Center of Excellence for Innovation in Chemistry (PERCH-CIC), Office of the Higher Education Commission, Ministry of Education, Thailand, for its partial funding is also appreciated by P.S.

Data Availability Statement: Not applicable.

Conflicts of Interest: No conflicts of interest are disclosed by the authors.

 doi:10.20944/preprints202409.1442.v

References

1. Elsheekh, K.M.; Kamel, R.R.; Elsherif, D.M.; Shalaby, A.M.; Achieving Sustainable Development Goals from the Perspective of Solid Waste Management Plans. *J. Eng. Appl. Sci.*, **2021**, *68*, 9.
2. Ruamcharoen, J.; Munlee, R.; Vayachuta, L.; Ruamcharoen, P; Bio-based Composites of Sago Starch and Natural Rubber Reinforced with Nanoclays. *Express Polym. Lett*. **2023**, *17*, 1096-1109.
3. Moshood, T.D.; Nawanir, G.; Mahmud, F.; Mohamad, F.; Ahmad, M.H.; Abdulghani, A.; Biodegradable Plastic Applications towards Sustainability: A Recent Innovations in the Green Product. *Clean. Eng.Technol*. **2022,** *6*, 100404.
4. Gupta, V.; Biswas, D.; Roy, S.; A Comprehensive Review of Biodegradable Polymer-based Films and Coatings and their Food Packaging Applications. *Materials* **2022**, *15*, 5899.
5. Onyeaka, H.; Obileke, K.; Makaka, G.; Nwokolo, N.; Current Research and Applications of Starch-based Biodegradable Films for Food Packaging. *Polymers* **2022**, *14*, 1126.
6. Mangaraj, S.; Yadav, A.; Bal, L.M.; Dash, S.K.; Mahanti, N.K.; Application of Biodegradable Polymers in Food Packaging Industry: A Comprehensive Review. *J. Packag. Technol. Res*. **2019**, *3*, 77-96.
7. Chavan, P.; Sinhmar, A.; Sharma, S.; Dufresne, A.; Thory, R.; Kaur, M.; Sandhu, K.S.; Nehra, M.; Vikash, N.; Nanocomposite Starch Films: A New Approach for Biodegradable Packaging Materials. *Starch* **2022**, *74*, 2100302.
8. Wannaphatchaiyong, S.; Suksaeree, J.; Waiprib, R.; Kaewpuang, A.; Saelee, W.; Pichayakorn, W.; Gelatin/Gelatinized Sago Starch Biomembranes as a Drug Delivery System Using Rubber Latex as Plasticizer. *J. Polym. Environ.* **2019**, *27*, 2380-2394.
9. Shah, S.A.; Sohail, M.; Khan, S.; Minhas, M.U.; Matas, M.de; Sikstone, V.; Hussain, Z.; Abbasi, M.; Kousar, M.; Biopolymer-Based Biomaterials for Accelerated Diabetic Wound Healing: A Critical Review. *Int. J. Biol. Macromol.* **2019**, *139*, 975-993.
10. Jonoobi, M.; Oladi, R.; Davoudpour, Y.; Oksman, K.; Dufresne, A.; Hamzeh, Y.; Davoodi, R.; Different Preparation Methods and Properties of Nanostructured Cellulose from Various Natural Resources and Residues: a Review. *Cellulose* **2015**, *22*, 935-969.
11. Lee, K.; Jeon, Y.; Kim, D.; Kwon, G.; Kim, U.-J.; Hong, C.; Choung, J.W.; You, J.; Double-Crosslinked Cellulose Nanofiber-Based Bioplastic Films for Practical Applications. *Carbohydr. Polym.* **2021**, *260*, 117817.
12. Filippo, M.F.D.; Dolci, L.S.; Liccardo, L.; Bigi, A.; Bonvicini, F.; Gentilomi, G.A.; Passerini, N.; Panzavolta, S.; Albertini, B.; Cellulose Derivatives-Snail Slime Films: New Disposable Eco-Friendly Materials for Food Packaging. *Food Hydrocoll.* **2021**, *111*, 106247.
13. Cazón, P.; Velázquez, G.; Vázquez, M.; Bacterial Cellulose Films: Evaluation of the Water Interaction. *Food Packag. Shelf Life* **2020**, *25*, 100526.
14. Liu, X.; Xiao, W.; Ma, X.; Huang, L.; Ni, Y.; Chen, L.; Ouyang, X.; Li, J.; Conductive Regenerated Cellulose Film and Its Electronic Devices- A Review. *Carbohydr. Polym.* **2020**, *250*, 116969.
15. Xie, X.; Liu, L.; Zhang, L.; Lu, A.; Strong Cellulose Hydrogel as Underwater Superoleophobic Coating for Efficient Oil/Water Separation. *Carbohydr. Polym.* **2020**, *229*, 115467.
16. Liu, X.; Xiao, W.; Ma, X.; Huang, L.; Ni, Y.; Chen, L.; Ouyang, X.; Li, J.; Conductive Regenerated Cellulose Film and Its Electronic Devices- A Review. *Carbohydr. Polym.* **2020**, *250*, 116969.
17. Wang, T.; Zhao, Y.; Optimization of Bleaching Process for Cellulose Extraction from Apple and Kale Pomace and Evaluation of Their Potentials as Film Forming Materials. *Carbohydr. Polym.* **2021**, *253*, 117225.
18. Baghaei, B.; Mikael Skrifvars, M.; All-Cellulose Composites: A Review of Recent Studies on Structure, Properties and Applications. *Molecules* **2020**, *25*(12), 2836.
19. Liu, Y.; Ahmed, S.; Sameen, D.E.; Wang, Y.; Lu, R.; Dai, J.W.; Li, S.; Qin, W.; A Review of Cellulose and Its Derivatives in Biopolymer-Based for Food Packaging Application. *Trends Food Sci. Technol*. **2021**, *112*, 532-546.
20. Yu, Z.; Dhital, R.; Wang, W.; Sun, L.; Zeng, W.; Mustapha, A.; Lin, M.; Development of Multifunctional Nanocomposites Containing Cellulose Nanofibrils and Soy Proteins as Food Packaging Materials. *Food Packag. Shelf Life*. **2019**, *21*, 100366.
21. Jiang, Z.; Ho, S.-H.; Wang, X.; Li, Y.; Wang, C.; Application of Biodegradable Cellulose-Based Biomass Materials in Wastewater Treatment. *Environ. Pollut.* **2021**, *290*, 118087.
22. Huang, M.; Tang, Y.; Wang, X.; Zhu, P.; Chen, T.; Zhou, Y.; Preparation of Polyaniline/Cellulose Nanocrystal Composite and Its Application in Surface Coating of Cellulosic Paper. *Prog. Org. Coat.* **2021**, *159*, 106452.
23. Joseph, B.; Sagarika V.K.; Sabu, C.; Kalarikkal, N.; Thomas, S.; Cellulose Nanocomposites: Fabrication and Biomedical Applications. *J. Bioresour. Bioprod.* **2020**, *5*, 223-237.
24. Altman, G. H.; Diaz, F.; Calabro, C.T. J.; Horan, R.L.; Chen, J.; Lu, H.; Richmond, J.; Kaplan, D.L.; Silk-based Biomaterials.
Biomaterials **2003**, *24*, 401-416.
25. Zhang, Y.Q.; Applications of Natural Silk Protein Sericin in Biomaterials. *Biotechnol. Adv.* **2002**, *20*, 91-100.

26. Meinel, L.; Hofmann, S.; Karageorgiou, V.; Kirker-Head, C.; McCool, J.; Gronowicz, G.; Zichner, L.; Langer, R.; Vunjak-Novakovic, G.; Kaplan, D.L.; 2005. The Inflammatory Responses to Silk Films *in vitro* and *in vivo*. *Biomaterials* **2005**, *26*, 147-155.
27. Srisuwan, Y.; Baimark, Y.; Srihanam, P.; Preparation of Regenerated Silk Sericin/Silk Fibroin blend Microparticles by Emulsification-Diffusion Method for Controlled Release Drug Delivery. Particul. Sci. Technol. **2017**, *35*, 387-392.
28. Wani, S.U.D.; Gautam, S.P.; Qadrie, Z.L.; Gangadharappa, H.V.; Silk Fibroin as a Natural Polymeric based Bio-Material for Tissue Engineering and Drug Delivery Systems-A Review. *Int. J. Biol. Macromol.* **2020**, *163*, 2145-2161.
29. Radulescu, D.-M.; Andronescu, E.; Vasile, O.R.; Ficai, A.; Vasile, B.S.; Silk Fibroin-based Scaffolds for Wound Healing Applications with Metal Oxide Nanoparticles. *J. Drug Deliv. Sci. Technol*. **2024**, *96*, 105689.
30. Srisuwan, Y.; Srihanam, P.; Preparation and Characterization of Keratin/Alginate blend Microparticles. *Adv. Mater. Sci. Eng*. **2018**, *2018*, 1-6.
31. Baimark, Y., Srisa-ard, M.; Srihanam, P.; Preparation of Bovine Serum Albumin Hollow Microparticles by the Water-in-Oil Emulsion Solvent Diffusion Technique for Drug Delivery Applications. *J. Chem. Soc. Pak*. **2012**, *34*, 131-134.
32. Srihanam, P.; Srisuwan, Y.; Imsombut, T.; Baimark, Y.; Silk Fibroin Microspheres Prepared by the Water-in-Oil Emulsion Solvent Diffusion Method for Protein Delivery. *Korean J. Chem. Eng*. **2011**, *28*, 293-297.
33. Phromsopha, T.; Srihanam, P.; Baimark, Y.; Preparation of Cross-linked Starch Microparticles by a Water-in-Oil Emulsion Solvent Diffusion Method for Use as Drug Delivery Carriers. *Asian J. Chem*. **2012**, *24*, 285-287.
34. Wongnarat, C.; Srihanam, P.; Biomaterial Microparticles of Keratose/Collagen blend Prepared by a Water-in-Oil Emulsification-Diffusion Method. *Particul. Sci. Technol*. **2020**, *31*, 379-384.
35. Imsombut, T.; Srisa-ard, M.; Srihanam, P.; Baimark, Y.; Preparation of Silk Fibroin Microspheres by Emulsification-Diffusion Method for Controlled Release Drug Delivery Applications. *E-Polymers*, 2011, 88, 1-8.
36. Thongsomboon, W.; Baimark, Y.; Srihanam, P.; Valorization of Cellulose-based Materials from Agricultural Waste: Comparison Between Sugarcane Bagasse and Rice Straw. *Polymers*, **2023**, *15*, 3190.
37. Wen, Y.; Liu, J.; Jiang, L.; Zhu, Z.; He, S.; He, S.; Shao, W.; Development of Intelligent/Active Food Packaging Film Based on TEMPO-Oxidized Bacterial Cellulose Containing Thymol and Anthocyanin-Rich Purple Potato Extract for Shelf Life Extension of Shrimp. *Food Packag. Shelf Life* **2021**, *29*, 100709.
38. Qi, Y.; Lin, S.; Lan, J.; Zhan, Y.; Guo, J. Fabrication of Super-High Transparent Cellulose Films with Multifunctional Performances via Post-Modification Strategy. *Carbohydr. Polym.* **2021**, *260*, 117760.
39. Karatzos, S.K.; Edye, L.A.; Orlando, W.; Doherty, S.; Sugarcane Bagasse Pretreatment Using Three Imidazolium - based Ionic Liquids: Mass Balances and Enzyme Kinetics. *Biotechnol. Biofuels* **2012**, *5*, 1-12.
40. Li, B.; Sun, Y.; Yao, J.; Wu, H.; Shen, Y.; Zhi, C.; Li, J. An Environment-Friendly Chemical Modification Method for Thiol Groups on Polypeptide Macromolecules to Improve the Performance of Regenerated Keratin Materials. *Mater. Des.* **2022**, *217*, 110611.
41. Biswas, S.; Rahaman, T.; Gupta, P.; Mitra, R.; Dutta, S.; Kharlyngdoh, E.; Guha, S.; Ganguly, J.; Pal, A.; Das, M.; Cellulose and Lignin Profiling in Seven, Economically Important Bamboo Species of India by Anatomical, Biochemical, FTIR Spectroscopy and Thermogravimetric Analysis. *Biomass Bioenerg*. **2022**, *158*, 106362.
42. Lassoued, M.; Crispino, F.; Loranger, E.; Design and Synthesis of Transparent and Flexible Nanofibrillated Cellulose Films to Replace Petroleum-Based Polymers. *Carbohydr. Polym*. **2021**, *254*, 117411.
43. Sharma, S.; Chatterjee, S.; Microplastic Pollution, a Threat to Marine Ecosystem and Human Health: A Short Review. *Environ. Sci. Pollut. Res*. **2017**, *24*, 21530-21547.
44. Pakkaner, E.; Yalçın, D.; Uysal, B.; Top, A.; Self - Assembly Behavior of the Keratose Proteins Extracted from Oxidized *Ovis aries* Wool Fibers. *Int. J. Biol. Macromol*. **2019**, *125*, 1008-1015.
45. Liu, Q.; Ying, G.; Jiang, N.; Yetisen, A.K.; Yao, D.; Xie, X.; Fan, Y.; Liu, H.; Three-Dimensional Silk Fibroin Microsphere-Nanofiber Scaffolds for Vascular Tissue Engineering. *Med. Nov. Technol. Devices* **2021**, *9*, 100051.
46. Huang, X.; Fu, Q.; Deng Y.; Wang, F.; Xia, B.; Chen, Z.; Chen, G.; Surface Roughness of Silk Fibroin/Alginate Microspheres for Rapid Hemostasis *In Vitro* and *In Vivo*. *Carbohyd. Polym.* **2021**, *253*, 117256.
47. Hidayati, S.; Zulferiyenni.; Maulidia, U.; Satyajaya, W.; Hadi, S.; Effect of Glycerol Concentration and Carboxy Methyl Cellulose on Biodegradable Film Characteristics of Seaweed Waste. *Heliyon* **2021**, *7*, e077.

 doi:10.20944/preprints202409.1442.v

48. Osorio-Ruiz, A.; Avena-Bustillos, R. J.; Chiou, B.-S.; Rodríguez-González, F.; MartinezAyala, A.-L.; Mechanical and Thermal Behavior of Canola Protein Isolate Films as Improved by Cellulose Nanocrystals. *ACS Omega* **2019**, *4*(21), 19172-19176.
49. Rojas-Lema, S.; Nilsson, K.; Trifol, J.; Langton, M.; Gomez-Caturla, J.; Balart, R.; Garcia-Garcia, D.; Morina, R.; Faba Bean Protein Films Reinforced with Cellulose Nanocrystals as Edible Food Packaging Material. *Food Hydrocoll.* **2021**, *121*, 107019.